The International Journal of Advanced Manufacturing Technology (2021) 114:2019–2030
https://doi.org/10.1007/s00170-021-06992-w

ORIGINAL ARTICLE

Experimental study on uniformity of copper layer with microstructure arrays by electroforming

Yongfei Zhao [1] · Shuangqing Qian [1] · Yong Zhang [2] · Xiaofeng Wan [1] · Hua Zhang [1]

Received: 30 October 2020 / Accepted: 22 March 2021 / Published online: 5 April 2021
© The Author(s), under exclusive licence to Springer-Verlag London Ltd., part of Springer Nature 2021

Abstract
Metal microstructures have a high potential to meet high application requirement of a variety of new industries because they can make components obtain optical, thermal, bionic, and other functional properties. Electroforming is one of the most efficient technologies for large-scale fabrication of micromachined devices with microstructures due to its good repeatability and reproducibility. However, the thickness nonuniformity of the electroformed layer is a bottleneck problem in the preparation of microstructures, which leads to quality defects such as voids in the microstructures. In order to fabricate the void-free microstructures, pulse electrodeposition of copper was proposed in this paper. The effects of pulse electrodeposition parameters on the surface morphology and thickness uniformity of copper deposits were investigated. In this paper, copper was electrodeposited by direct current and pulse current respectively on the microgroove arrays with an aspect ratio of 2.5:1. The experimental results revealed that the pulse parameters can effectively improve the quality of the electroformed layer and enhance the uniformity of the microgrooves. It was determined that the pulse average current density 2 A/dm^2, the duty cycle 20%, and the frequency 2000 Hz were the optimum parameters for copper electroforming. Under these conditions, the void-free microstructures were successfully prepared.

Keywords Microstructures · Electroforming · Copper · Pulse parameters · Uniformity

1 Introduction

Products with microstructure arrays, such as corrugated horns, microchannel heat exchangers, and hydrophobic films, have great market potential in communication, heat transfer, biomedicine, and other fields [1–3]. The introduction of surface microstructure arrays can enable these devices to perform specific physical and chemical functions [4]. Fabrication methods for surface microstructure arrays have attracted extensive attention due to the increasing demand for minute and novel functional devices in various fields. Nevertheless, the traditional processing methods are not well suited for mass production because of their high fabrication costs and low throughput. Hence, it is essential to explore a new method for the fabrication of the microstructures.

The commercialization of microcomponents requires a low-cost, high-effectivity, high-precision fabrication technique [5–7]. Electroforming is one of the processes that might satisfy these requirements. In comparison with traditional metal processing technology, electroforming can reduce the number of processes from blank to parts with microstructures [8]. However, the problems of the difficulties of mass transfer, edge effect, cathodic polarization, and so on can occur in the process of electroforming, which result in the growth rate of the electroformed layer at the top edge of the microstructures that is faster than that at the bottom edge [9–11]. Thus, the void defects shown in Fig. 1 are formed in the microstructures. For these reasons, several attempts have been made to improve the uniformity of the electroformed layer, so as to fabricate the void-free microstructures.

With regard to the improvement of ion mass transfer, Zhao et al. [12] established a common computational model based on mass transfer coefficient for quantitative study of the mass transfer in megasonic microelectroforming. Both the simulation and experimental results showed that megasonic agitation enhanced

✉ Shuangqing Qian
sqqian@ntu.edu.cn

[1] School of Mechanical Engineering, Nantong University, Nantong 226019, China

[2] Department of Mechanical and Electrical Engineering, Shazhou Professional Institute of Technology, Zhangjiagang 215600, China

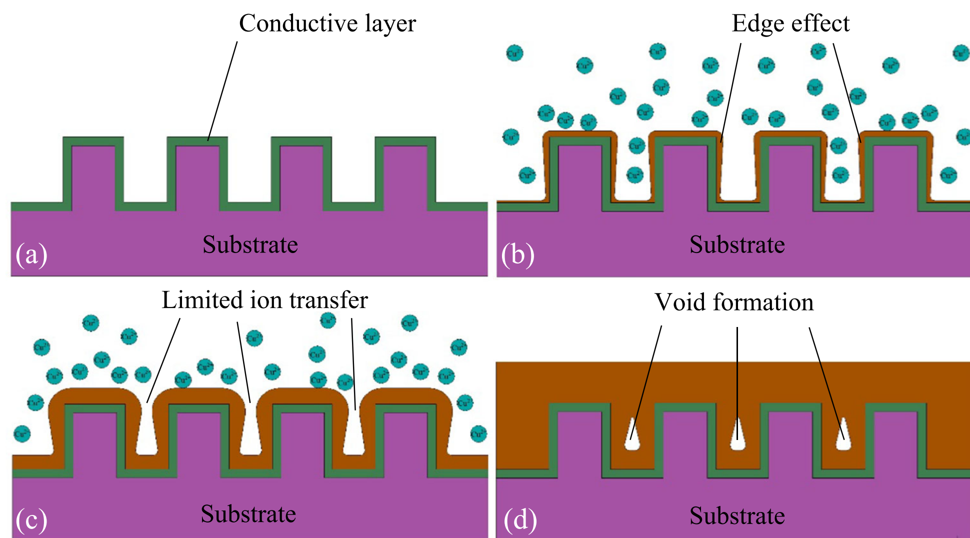

Fig. 1 **a**–**d** Schematic diagram of the formation of voids between microstructures during the electroforming process

the mass transport in microelectroforming. In addition, mass transfer coefficient was inversely proportional to the aspect ratio and distance between microchannel and transducer. Ming et al. [13] investigated the effects of vacuum degassing technology and surface boiling technology on electroforming. The results showed that vacuum boiling electroforming enhanced the mass transfer of electrolyte and then improved surface quality of the deposited layer. Sun et al. [14] investigated the effect of pulsed magnetic field on Ni-SiC composite coating. The results showed that magnetic field can affect the mass transfer of solute and effectively improve the quality of Ni-SiC composite coating.

Besides, the optimization of cathode electric field distribution is also helpful for improving the uniformity of the electroformed layer. Haghdoost et al. [15] systematically studied the influence of applied voltage and micromold geometry on the electrodeposition of microgrooves by numerical simulation. Jiang et al. [16] adopted a nonconducting shield, a secondary electrode, and a movable cathode to improve the thickness uniformity of nickel deposits. The experimental results indicated that the three methods can effectively improve the thickness uniformity of nickel deposits. Zhu et al. [17] used auxiliary cathode to restrain the overgrowing on the cathode boundary. Both results of simulation and experiments proved the positive effects of auxiliary cathode.

Furthermore, Xue et al. [18] studied the effect of pulse duty cycle on the quality of nanocrystalline Ni-GO composite coatings by supercritical CO_2-assisted pulse electrodeposition. The study of duty cycle suggested that the off-time was beneficial to improve the thickness uniformity. Feng et al. [19] built a threefold diffusion layer model for the pulse reverse nanoelectroforming. The model revealed that that pulse reverse electroforming was easier to replenish metallic ions in pulsating diffusion layer than pulse electroforming when the pulse current was turned off, which further improved the uniformity of the electroformed layer. Wang et al. [20] changed the concentration of additives and the process parameters of pulse reverse plating to improve the uniformity of copper plating through holes. Chen et al. [21] used the oscillating method and the additive with synergistic effect to form a uniform copper layer. Xiao et al. [22] simulated the effect of additives on the filling of through-silicon via (TSV) and obtained three different simulation results, which were consistent with the experimental results. Under appropriate conditions, the TSV with diameter of 20 μm and depth of 200 μm was completely filled.

The aim of this work is to eliminate the voids in the microstructure arrays to achieve high-performance copper deposits. In this study, the effects of pulse current density, duty cycle, and frequency on the surface morphology and thickness uniformity of copper deposits were systematically evaluated. Based on this, the optimal machining parameters for electroforming experiment were obtained. Besides, the void-free microstructures were fabricated by pulse electroforming to prove the feasibility of this method.

2 Experimental procedures

2.1 Microgroove preparation process

Figure 2 demonstrates a schematic illustration of the fabrication process for the creation of the metal microstructures. The specific experimental process is as follows: First, the nonmetal substrate with high-aspect-ratio microgrooves on the surface is fabricated by using 3D printing technology. Furthermore, a conductive layer is applied to the surface of the nonmetal substrate before electroforming to facilitate copper deposition. Subsequently, the electrodeposition is stopped when the electroformed layer reaches a certain thickness. Finally, the sample with microstructure arrays is put into acetone solution to dissolve the substrate so as to obtain a complete electroformed layer.

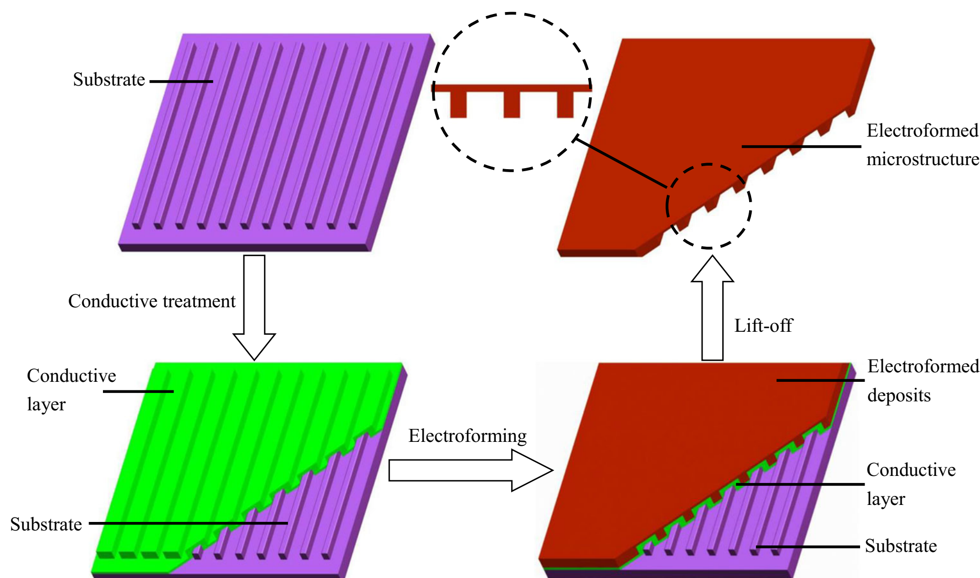

Fig. 2 Outline of the steps involved in fabricating the metal microstructure using electroforming technology

2.2 Electroforming experimental equipment

The self-designed electroforming equipment is shown in Fig. 3. During electroforming process of microgroove structures, an electrodeposition system mainly includes a water circulation system, an anode plate, a cathode plate, an electroforming bath, a magnetic stirrer, a temperature controller, and a power supply. A water circulation system consists of a flow meter, a ball valve, a filter, a pump, and an overflow valve. The temperature controller kept the solution temperature constant. A phosphor bronze plate was used as the anode. The cathode was made of photosensitive resin substrate with the exposed area of 20 mm × 30 mm and the other area was insulated. The substrate used was fabricated by stereolithography apparatus (SLA) and its surface precision can reach ± 0.1 mm. The substrate surface was brushed with a commercial silver conductive paint (MECHANIC Supplies) to facilitate copper deposition. The anode and cathode were positioned vertically and face to face with each other in the plating solution. The distance between anode and cathode was fixed with 30 mm. The cathode diagram is shown in Fig. 4a. From the cross-section P shown in Fig. 4b, the structural dimensions of the microgrooves on the substrate surface can be obtained, where $h = 750$ μm, $w_1 = 500$ μm, $w_2 = 300$ μm, and $R = 50$ μm.

2.3 Electrolyte and characterizations

Taking the properties of the electroformed layer into consideration, pyrophosphate bath is the best choice for the electroforming process. Bath composition and electrodeposition parameters are listed in Table 1. Both direct current and

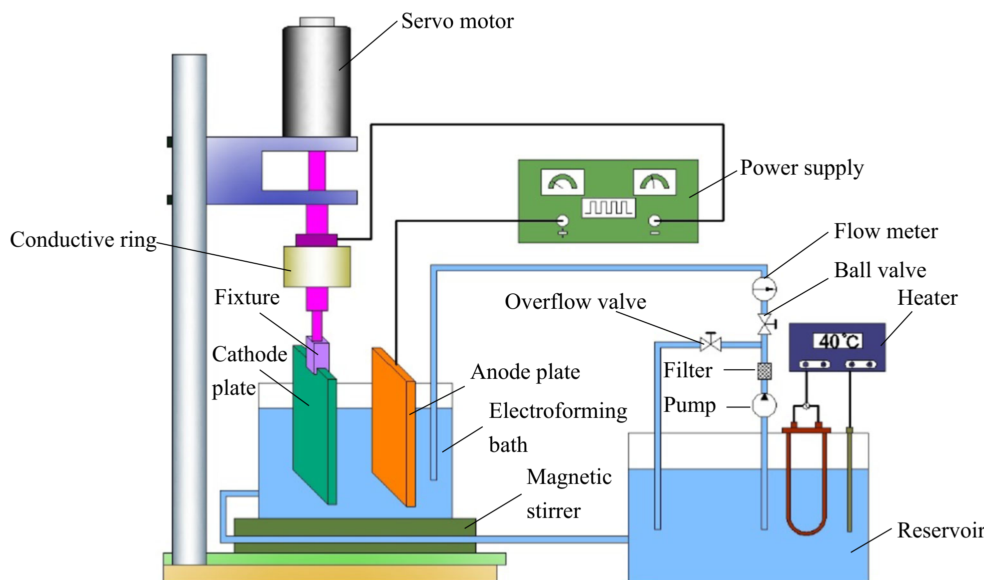

Fig. 3 Schematic diagram of the electroforming equipment

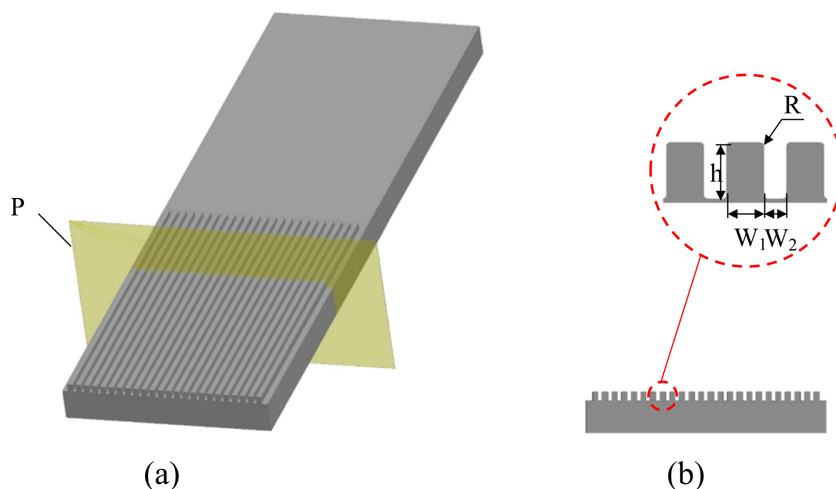

Fig. 4 Model of microgrooves. **a** Diagram. **b** Section

pulse current were used in the experiments. The electrolyte solution was prepared using deionized water. The pH of the solution was maintained at 8–9 using either $NH_3{\cdot}H_2O$ or $H_4P_2O_7$ solutions. Before electroforming, sulfuric acid and deionized water were used to clean the cathode surface to ensure the quality of the electroformed layer. Evaluation of deposit morphology was carried out by SEM typing JSM-6510, made by JEOL Ltd., and metallurgical microscope typing FM-JX100A, made by FSM-Precision Ltd. In order to ensure the reliability of the experimental data, the samples were prepared three times, and each group of sample data was measured three times. On this basis, the average value was taken.

3 Results and discussion

In the experiment, metal microstructures with a pitch of 0.8 mm and a height of 0.75 mm were fabricated by direct current and pulse current electroforming. In this study, the surface topography and cross-sectional morphology of the copper layers prepared by different electroforming processes were compared. The optimum operation parameters of the copper deposits formed by PC electroforming were identified. In this condition, the void-free microstructure was fabricated. The results and discussion are presented as follows.

Table 1 Electrolyte composition and electrodeposition conditions

Bath constituent or electrodeposition conditions	Amount or conditions
$Cu_2P_2O_7$ (copper(II) pyrophosphate)	70 g/L
$K_4P_2O_7$ (potassium pyrophosphate)	300 g/L
$NH_3{\cdot}H_2O$	2–3 mL/L
Average current density	1, 2, 3, 4 A/dm^2
Duty cycle	20%, 40%, 60%, 80%
Frequency	500, 1000, 2000, 3000 Hz
Temperature	40 °C
pH	8–9

3.1 Influence of current density on the electroformed layer

Figure 5 is the SEM micrographs of the surface of the copper electrodeposits, which are obtained under direct current densities of 1, 2, 3, and 4 A/dm^2, respectively. The nucleation rate and growth rate of grains affect the surface morphology of the electroformed layer. When the nucleation rate is greater than the growth rate, the grain size of the electroformed layer is refined. On the contrary, the grains become larger and the surface of the electroformed layer becomes rough. From the result, it was found that the grain size of copper deposits was refined and then increased. Under the condition of the direct current density of 1 A/m^2 and 2 A/dm^2, the surface of the electroformed layer was similar and smooth. The size of grains was finer and uniform. When the current density continued to increase, the grain size of copper deposits grew continuously. When the direct current density rose to 4 A/dm^2, the surface of the electrodeposits became uneven.

Figure 6 shows the surface morphologies of the copper electrodeposits obtained at pulse average current densities of 1, 2, 3, and 4 A/dm^2 when the pulse duty cycle and frequency were kept constant at 20% and 2000 Hz, respectively. It illustrated that a finer grain size was obtained when the pulse average current density increased from 1 to 2 A/dm^2. When the pulse average current density rose to 4 A/dm^2, the grains of the electroformed layer began to grow and become rough. At the current density of 2 A/dm^2, the electrodeposits became more uniform and compact.

On further increase of the current density, the results showed that the copper grains became coarser and the grain

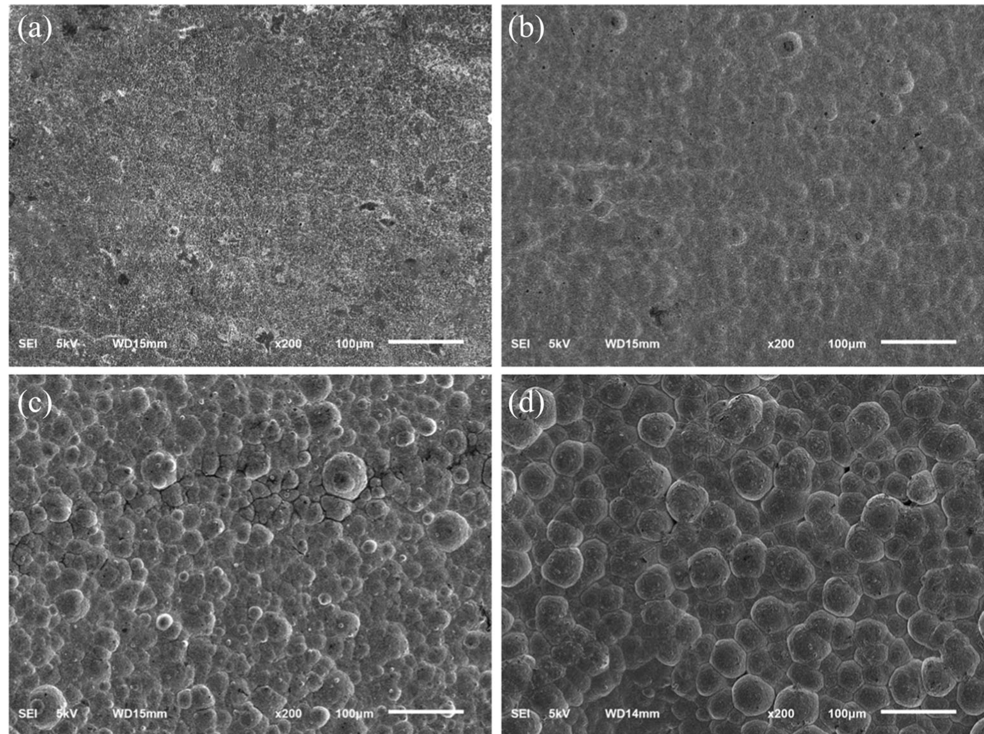

Fig. 5 SEM micrographs showing the effect of the direct current density on surface morphology. **a** 1 A/dm^2. **b** 2 A/dm^2. **c** 3 A/dm^2. **d** 4 A/dm^2

combination was loose. The grain sense was very obvious. The results showed that pinhole defects appeared on the surface of the electroformed layer, as shown in Fig. 7. A sponge-like electroformed layer was formed. The structure of copper deposits was loose and the compactness was poor. The strength and property of the electroformed layer were low and easy to fracture. It is known that with the increase of current density, the cathodic polarization and the cathodic overpotential increase accordingly. As a result, the nucleation rate of grains is increased and the critical radius of nucleation is reduced. Thus,

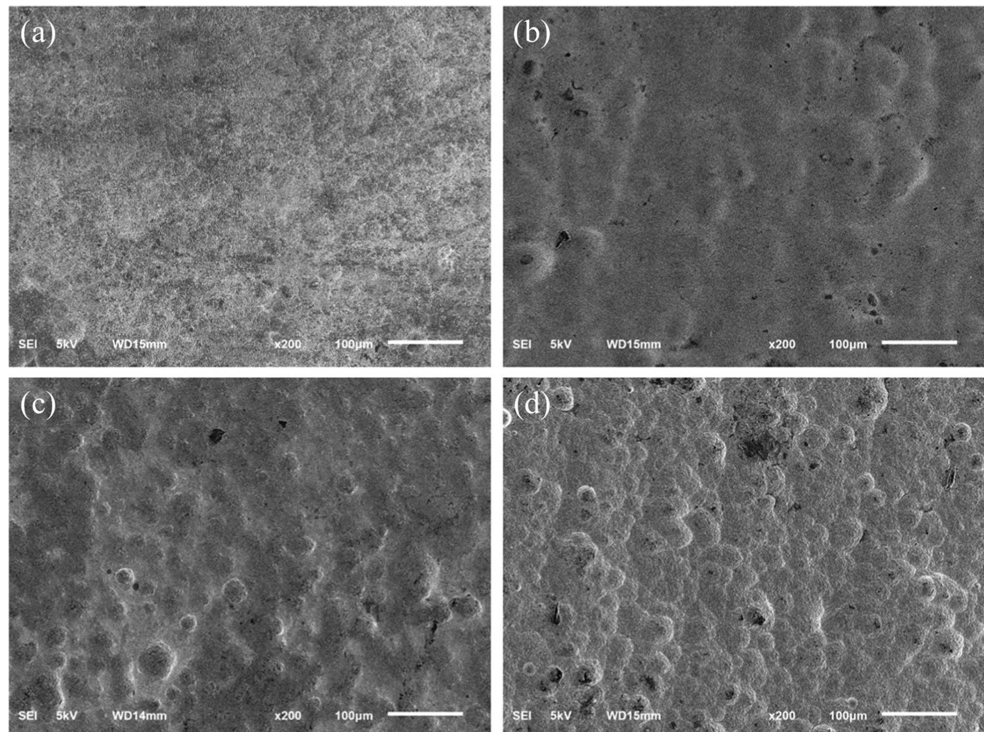

Fig. 6 SEM micrographs showing the effect of the pulse average current density on surface morphology. **a** 1 A/dm^2. **b** 2 A/dm^2. **c** 3 A/dm^2. **d** 4 A/dm^2

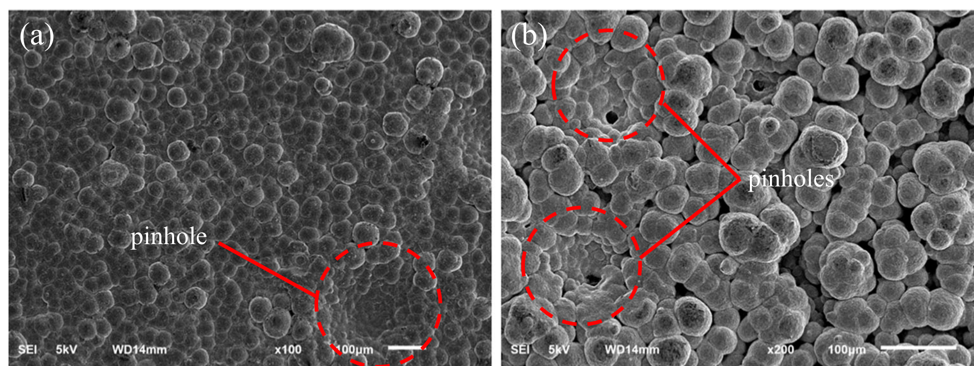

Fig. 7 SEM micrographs showing the effect of the high current density on surface morphology. **a** Direct current. **b** Pulse current

the grains in the electroformed layer are refined. However, when the current density is too high, the discharge metal ions near the cathode are seriously lacking, and the surface concentration polarization phenomenon is gradually obvious, which cause the electroformed layer to scorch or loose. As a result, the electroformed layer became brittle.

To characterize the uniformity of the metal microstructure thickness, thickness nonuniformity η is adopted. Its formula can be described as:

$$\eta = \frac{t_{\text{top}} - t_{\text{bottom}}}{t_{\text{bottom}}} \times 100\% \quad (1)$$

where t_{top} is the top edge thickness of the microstructures and t_{bottom} is the bottom edge thickness of the microstructures, respectively.

The thickness nonuniformities η with different direct current densities and pulse current densities are calculated and shown in Figs. 8 and 9.

As illustrated in Fig. 8, the results showed that that the nonuniformity η with direct current density of 1 A/dm^2 was higher than that of direct current density of 2 A/dm^2. When the direct current density increased to 4 A/dm^2, the nonuniformity of the copper electrodeposits was the highest. When the direct current density was 2 A/dm^2, the thickness of the electroformed layer was the most uniform, and the nonuniformity reached 248.4%. As shown in Fig. 10c, d, the electric field distribution was uneven due to the high current density. The grains of the copper were coarse. So the surface of the electroformed layer was uneven. It is consistent with the conclusion in Fig. 5.

It can be seen from Fig. 9 that the nonuniformities of the microstructure firstly decreased and then increased when the pulse average current density increased from 1 to 4 A/dm^2. When the pulse average current density was 2 A/dm^2, the thickness of the electroformed layer was the most uniform, and the nonuniformity reached 215.5%. Compared with DC electroforming with direct current density of 2 A/dm^2, the uniformity of the electroformed layer was improved by 13.2% when the pulse average pulse current density was 2 A/dm^2. Figure 11 shows the changes of microstructure at different current densities. Compared with Figs. 10 and 11, it was found that the microstructure thickness was more uniform and smooth under the condition of pulse current. Under the condition of pulse electroforming, the current density changes periodically, which promotes the metal ions to pass through the outer diffusion layer towards the cathode. So the electroformed layer becomes more uniform.

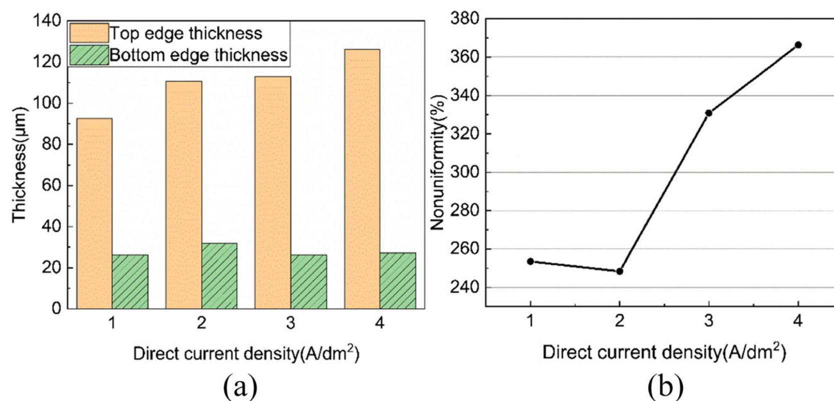

Fig. 8 The results of nonuniformities with different direct current densities. **a** The thicknesses of the electroformed layer. **b** The nonuniformities of the microgroove

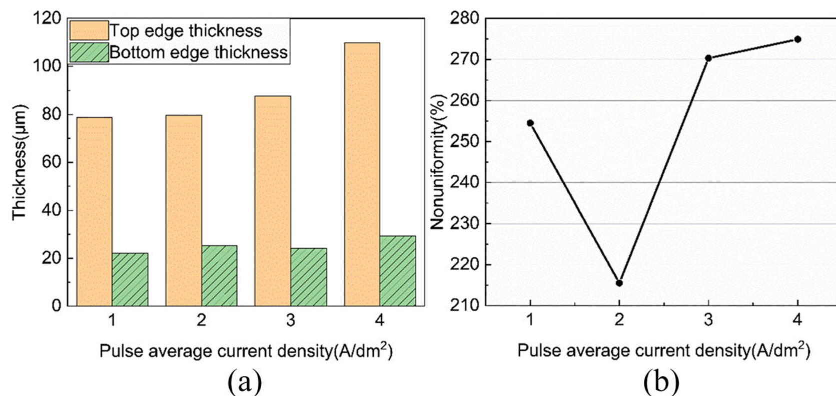

Fig. 9 The results of nonuniformities with different pulse average current densities. **a** The thicknesses of the electroformed layer. **b** The nonuniformities of the microgroove

3.2 Influence of duty cycle on the electroformed layer

Figure 12 demonstrates the surface morphologies of the copper electrodeposits obtained at duty cycle of 20, 40, 60, and 80%. Other parameters remain constant (the current density of 2 A/dm^2 and the frequency of 2000 Hz). When the duty cycle was 20%, the surface morphology of the electroformed layer was the most homogeneous and smooth. The grain size was finer. It shows that a finer grained, more uniform electroformed layer could be obtained with the reduction of duty cycle. A decrease in duty cycle would result in a decreased deposition time and increase of pause time. It can be concluded that with the decrease of duty cycle, the continuous growth time of grains in each pulse period is decreased. When the average current density is the same and the duty cycle is small, the peak current density is higher. The instantaneous higher current density increases the cathode overpotential, which reduces the critical nucleation radius of the electroformed layer. As a result, fine grains are formed. The results also confirmed this fact.

Nonuniformities of the electroformed layer under different duty cycles are shown in Fig. 13. It showed that the nonuniformity was decreased with the reduction of duty cycle. It is considered that the increase of duty cycle means the increase of on-time and the decrease of off-time. Due to the increase of duty cycle, the ion consumption rate near the cathode is much faster than the diffusion speed of ions, which has no time to transfer. At last, the concentration difference is produced.

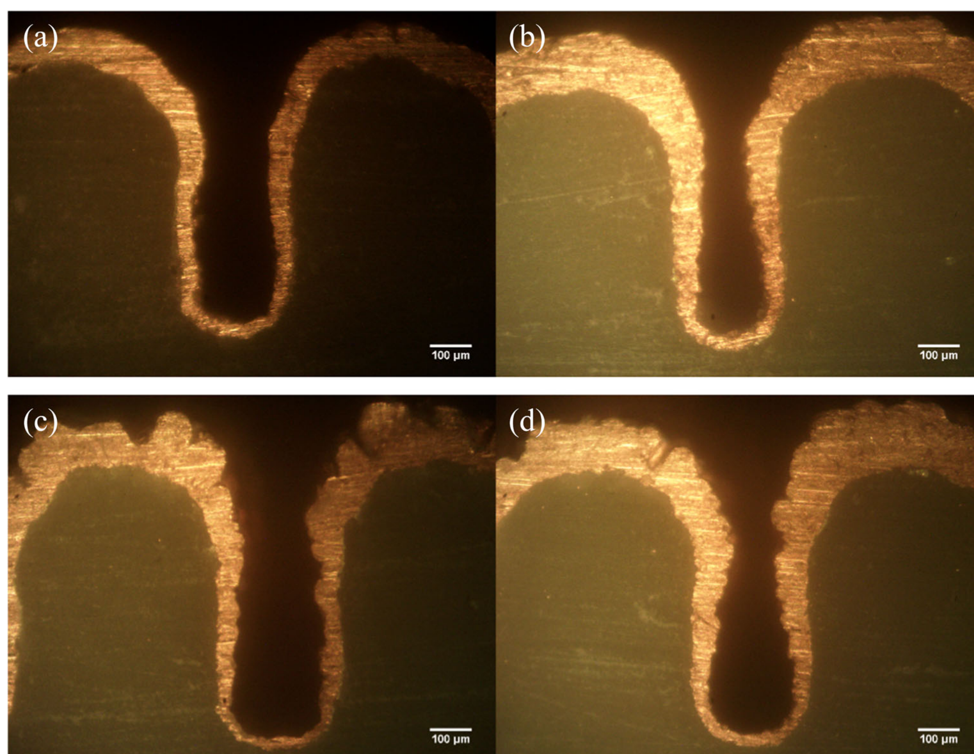

Fig. 10 Cross-section images of copper deposits produced by the different direct current densities. **a** 1 A/dm^2. **b** 2 A/dm^2. **c** 3 A/dm^2. **d** 4 A/dm^2

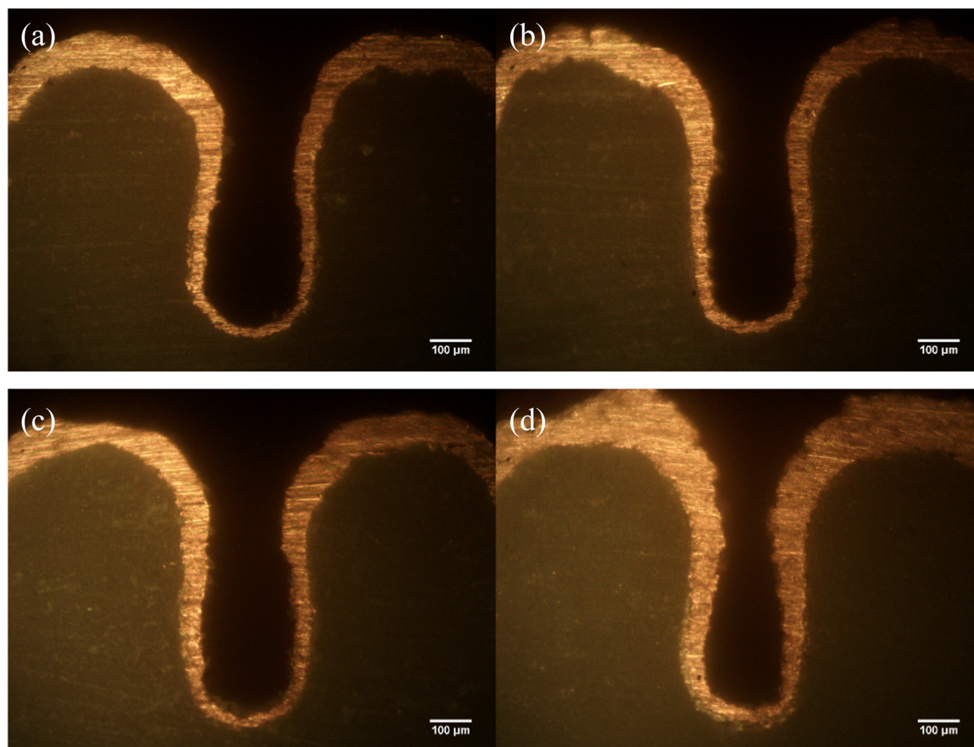

Fig. 11 Cross-section images of copper deposits produced by the different pulse average current densities. **a** 1 A/dm^2. **b** 2 A/dm^2. **c** 3 A/dm^2. **d** 4 A/dm^2

Hence, the increase of the duty cycle decreases the thickness uniformity of the copper deposits. The cross-section images are shown in Fig. 14. When the duty cycle was 80%, the thickness of the electroformed layer was the most uneven. In general, when the duty cycle decreased, the thickness of the top corners was getting thinner and thinner. When the duty

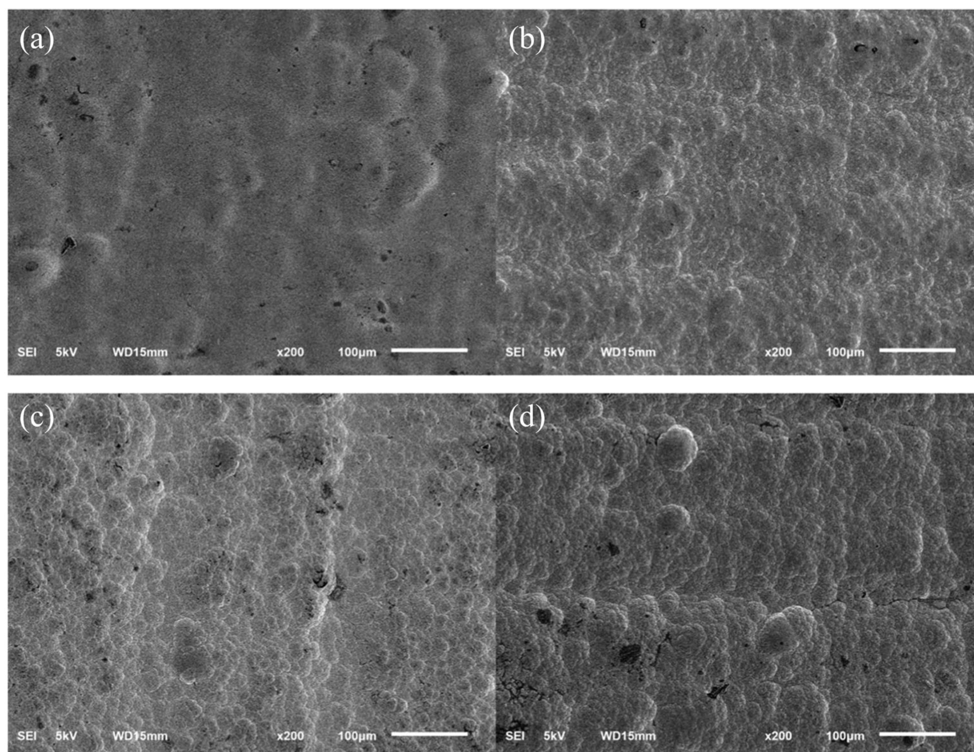

Fig. 12 SEM micrographs showing the effect of the duty cycle on surface morphology. **a** 20%. **b** 40%. c 60%. **d** 80%

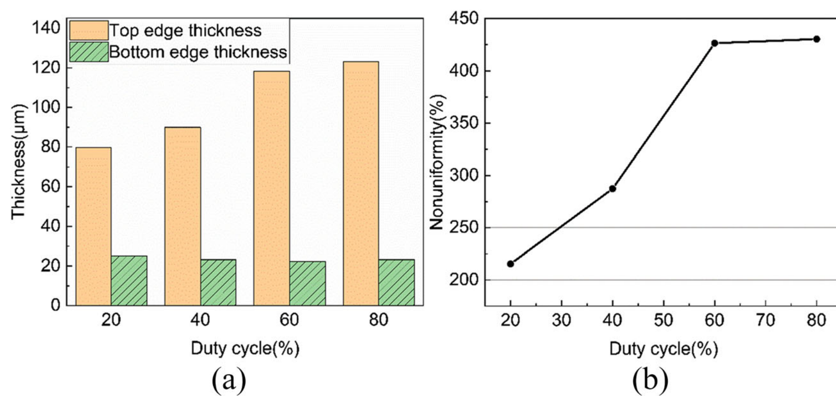

Fig. 13 The results of nonuniformities with different duty cycles. **a** The thicknesses of the electroformed layer. **b** The nonuniformities of the microgroove

cycle decreased from 60 to 20%, the thickness uniformity of the microstructure was increased by 0.9%, 33.2%, and 50%, respectively.

3.3 Influence of frequency on the electroformed layer

Figure 15 depicts the surface morphologies of the electroformed layer that have been achieved using various frequencies, respectively. The copper electrodeposits were obtained from the average current density of 2 A/dm^2 and the duty cycle of 20%. When the frequency increased to 2000 Hz, the surface of the copper deposits was the most uniform and smooth. The analysis results show that when the pulse frequency increase, the pulse period become shorter and the on-time cut down. The deposition time of copper in one cycle becomes shorter, which interrupts the continuous growth of grains and made the grains refined. When the frequency increased to 3000 Hz, the grains on the surface of the electroformed layer became coarse. The analysis illustrates that when the pulse frequency is too high, the influence of capacitance effect will become significant, thus losing the advantage of pulse, which is almost equal to DC electroforming.

Nonuniformities η of the deposits with different frequencies are displayed in Fig. 16. It can be seen that the nonuniformity of the microstructure was the lowest when the frequency was 2000 Hz. Figure 17 represents the cross-section morphology of electroformed layer at different frequencies. When the frequency is the lowest, the thickness of the

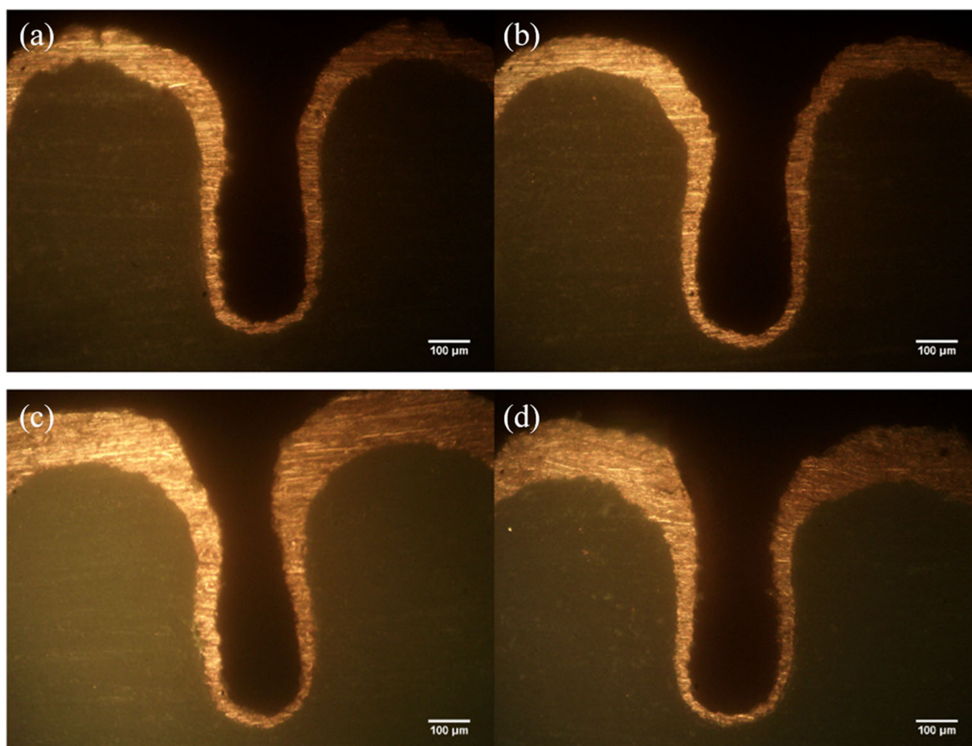

Fig. 14 Cross-section images of copper deposits produced by the different duty cycles. **a** 20%. **b** 40%. **c** 60%. **d** 80%

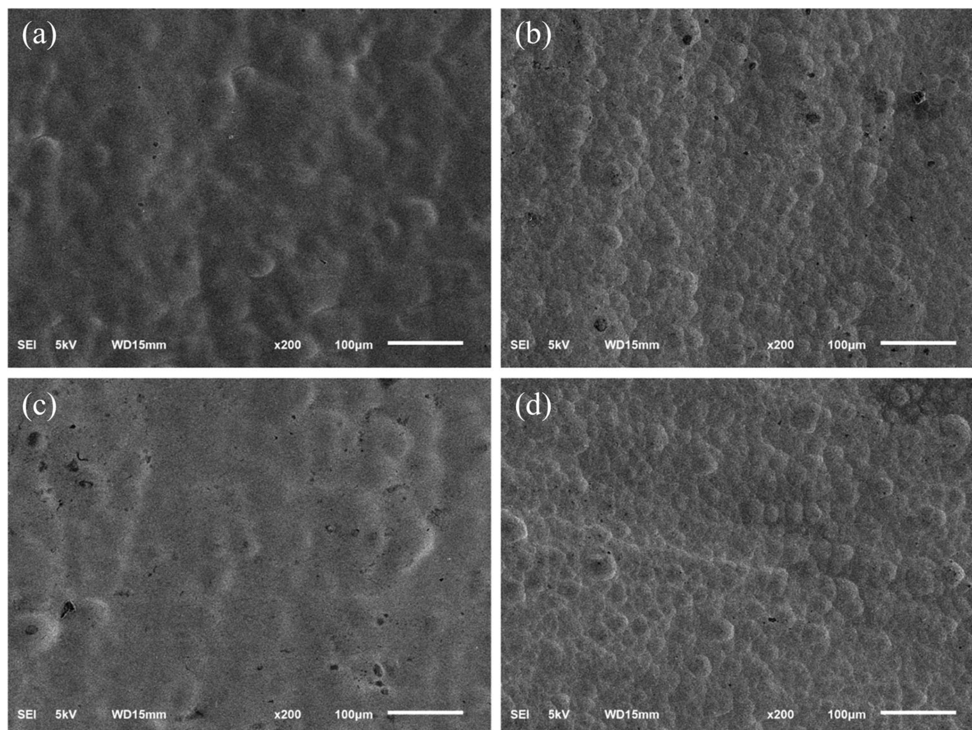

Fig. 15 SEM micrographs showing the effect of the frequency on surface morphology. **a** 500 Hz. **b** 1000 Hz. **c** 2000 Hz. **d** 3000 Hz

electroformed layer is more uneven. As can be seen from Fig. 16a, when the frequency was 500 Hz, the electroformed layer on the top edge of the microstructure was thicker than that at other frequencies. The results showed that the uniformity of the microstructure was improved by 34.1%, 36.4%, and 33.8% when the frequency increased from 1000 to 3000 Hz. The lower frequency means that the pulse period and the on-time increase, which leads to increasing the thickness of pulse diffusion layer.

4 Fabrication of the void-free microstructures

According to the analysis in Section 3, the pulse current can be used to improve the thickness uniformity. Thus, in order to verify the effectiveness of this method, the microstructures were fabricated by direct current and pulse current electroforming, respectively. Figure 18a displays the cross-section of the electroformed layer with void at direct current density of 2 A/dm^2. Figure 18b shows the microgroove without defects fabricated with a pulse average current density of 2 A/dm^2, a duty cycle of 20%, and a frequency of 2000 Hz. In the electroforming process of high-aspect-ratio microstructures, a high current distribution is concentrated at the top corners, resulting in the rapid growth of the copper electroformed layers. In this case, the top electrodeposition layers were closed, with voids remaining in the center. This phenomenon leads to the formation of voids in the electroformed layers, causing degradation of the sample performance. Compared with DC electroforming, pulse electroforming can change duty cycle and frequency, which makes copper ions intermittently deposit, reduces

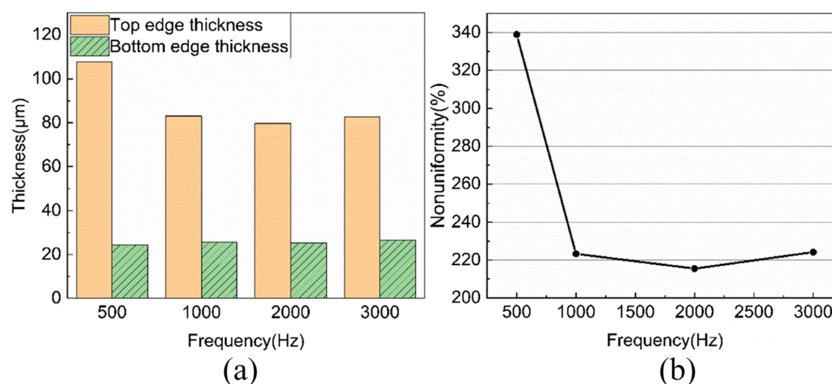

Fig. 16 The results of nonuniformities with different frequencies. **a** The thicknesses of the electroformed layer. **b** The nonuniformities of the microgroove

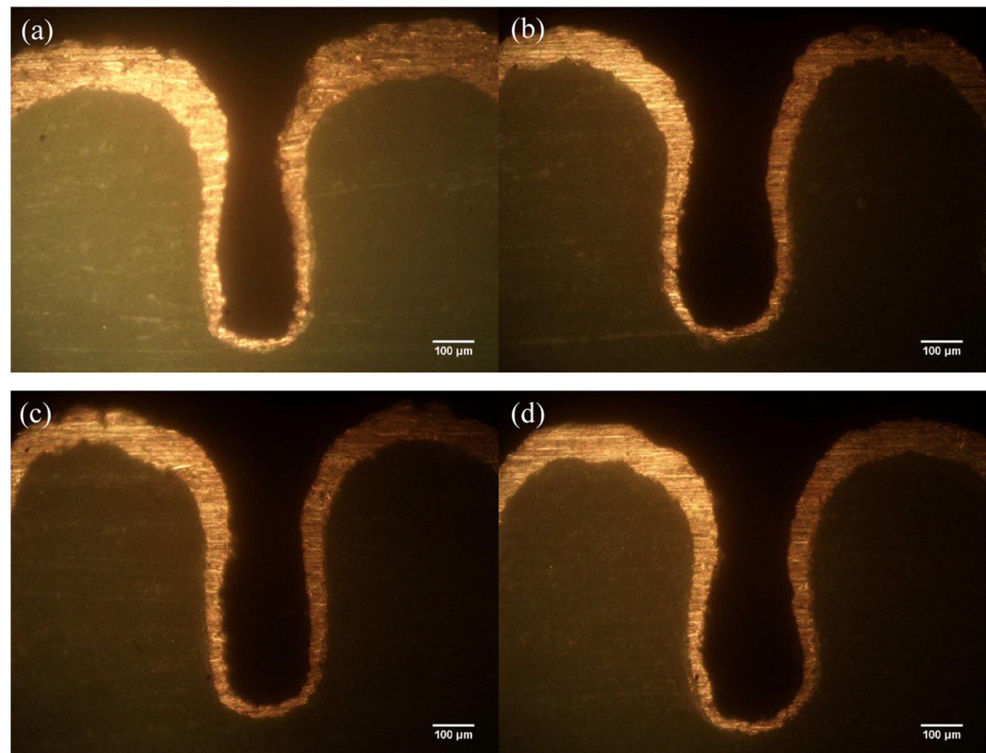

Fig. 17 Cross-section images of copper deposits produced by the different frequencies. **a** 500 Hz. **b** 1000 Hz. **c** 2000 Hz. **d** 3000 Hz

concentration polarization, and increases cathode overpotential. Therefore, pulse current can effectively improve the uniformity and quality of the electroformed layer.

5 Conclusions

In this study, electrodeposition experiments of the copper deposits were carried out in different current densities, duty cycles, and frequencies in order to obtain high uniformity and high-quality copper deposits. The effects of current density, duty cycle, and frequency on microstructure, texture, and uniformity of the copper deposits are studied and the results are as follows:

(1) Through experimental analysis, the grain size of the copper deposits is refined and then coarsened when the current density increases. Compared with direct current, pulse current can effectively refine the grain size and improve the uniformity of microstructure deposition.
(2) With the decrease of duty cycle, the deposition time decreases and the interruption time increases. So the ion diffusion layer becomes thinner and the cathode overpotential increases. The decrease of duty cycle can improve the uniformity and surface quality of the copper layers.
(3) In a certain range, when the pulse frequency increases, the electroformed layer is smoother, organization is more compact, and grains are finer. In addition, the thickness of casting layer is more uniform. However, when the

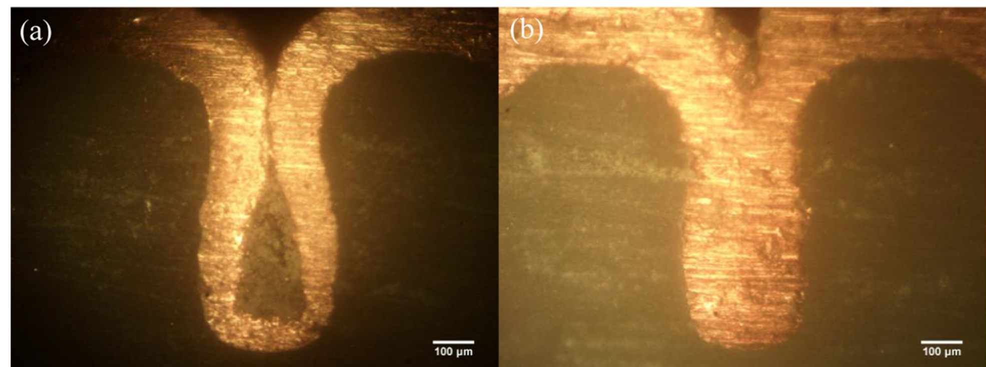

Fig. 18 Cross-section images of copper deposits. **a** Electroformed layer with void. **b** Electroformed layer without void

frequency is too high, the quality of electroforming decreases.

Author's contribution SQ contributed significantly to the conception of the study and revised the manuscript. YFZ performed the experiment, analyzed the experiment, and wrote the manuscript. YZ, XW, and HZ helped perform the analysis with constructive discussions.

Funding This work was financially supported by the National Natural Science Foundation of China (No. 51305212), the Priority Academic Program Development of Jiangsu Higher Education Institutions, and the Qing Lan Project of Jiangsu Province.

Data availability The datasets used or analysed during the current study are available from the corresponding author on reasonable request.

Code availability Not applicable.

Declarations

Conflict of interest The authors declare no competing interests.

References

1. Salimi T, Maghoul A, Abbasid AA (2013) Design of a compact Gaussian profiled corrugated horn antenna for low sidelobe-level applications. Int J Comput Theory Eng 5:223–226. https://doi.org/10.7763/IJCTE.2013.V5.682
2. Borquist E, Thapa S, Weiss L (2016) Experimental and lattice Boltzmann simulated operation of a copper micro-channel heat exchanger. Energy Conv Manag 117:171–184. https://doi.org/10.1016/j.enconman.2016.02.066
3. Weng C, Yang J, Wang F, Ding T, Zhai Z (2020) Thermodynamic analysis and injection molding of hierarchical superhydrophobic polypropylene surfaces. J Polym Eng 40(1):86–97. https://doi.org/10.1515/polyeng-2019-0109
4. Sugihara T, Enomoto T (2017) Performance of cutting tools with dimple textured surfaces: a comparative study of different texture patterns. Precis Eng 49:52–60. https://doi.org/10.1016/j.precisioneng.2017.01.009
5. Hernández-Castellano PM, Benítez-Vega AN, Díaz-Padilla N, Ortega-García F, Socorro-Perdomo P, Marrero-Alemán MD, Salguero J (2017) Design and manufacture of structured surfaces by electroforming. Procedia Manuf 13:402–409. https://doi.org/10.1016/j.promfg.2017.09.030
6. Li M, Liu J, Zhang X, Tian Y, Jiang K (2018) Fabrication of grapheme/nickel composite microcomponents using electroforming. Int J Adv Manuf Technol 96(9):3191–3196. https://doi.org/10.1007/s00170-018-1824-1
7. Pan CT, Chen YC, Wang SY, Cheng YT, Yen CK, Lin YL, Shih WC (2017) TSV by 355 UV laser for 4G component packaging with micro-electroforming. Microelectron Reliab 78:331–338. https://doi.org/10.1016/j.microrel.2017.09.023
8. Zhan X, Cao QD, Trieu K, Zhang X (2020) Microstructure and mechanical properties of copper microtubes fabricated via the electroforming process. J Mater Eng Perform 29(24):1741–1750. https://doi.org/10.1007/s11665-020-04691-3
9. Weng C, Zhou M, Jiang B, Lv H (2016) Improvement on replication quality of electroformed nickel mold inserts with micro/nano-structures. Int Commun Heat Mass Transf 75:92–99. https://doi.org/10.1016/j.icheatmasstransfer.2016.03.025
10. Solovjev DS, Solovjeva IA, Konkina VV, Litovka YV (2019) Improving the uniformity of the coating thickness distribution during electroplating treatment of products using multi anode baths. Mater Today: Proc 19:1895–1898. https://doi.org/10.1016/j.matpr.2019.07.036
11. Yamamoto T, Igawa K, Tang H, Chen C-Y, Chang T-FM, Nagoshi T, Kudo O, Maeda R, Sone M (2019) Effects of current density on mechanical properties of electroplated nickel with high speed sulfamate bath. Microelectron Eng 213:18–23. https://doi.org/10.1016/j.mee.2019.04.012
12. Zhao M, Du L, Du C, Wei Z, Ji X, Bai Z, Liu X (2019) Quantitative study of mass transfer in megasonic micro electroforming based on mass transfer coefficient: simulation and experimental validation. Electrochim Acta 297:328–333. https://doi.org/10.1016/j.electacta.2018.12.018
13. Ming P, Li Y, Wang S, Li S, Li X (2012) Microstructure and properties of nickel prepared by electrolyte vacuum boiling electrodeposition. Surf Coat Technol 213:299–306. https://doi.org/10.1016/j.surfcoat.2012.09.067
14. Sun C, Liu X, Zhou C, Wang C, Cao H (2019) Preparation and wear properties of magnetic assisted pulse electrodeposited Ni–SiC nanocoatings. Ceram Int 45(1):1348–1355. https://doi.org/10.1016/j.ceramint.2018.07.242
15. Haghdoost A, Pitchumani R (2011) Numerical analysis of electrodeposition in microcavities. Electrochim Acta 56(24):8260–8271. https://doi.org/10.1016/j.electacta.2011.06.084
16. Jiang B-Y, Weng C, Zhou M-Y, Lv H, Dietmar D (2016) Improvement of thickness deposition uniformity in nickel electroforming for micro mold inserts. J Cent South Univ 23:2536–2541. https://doi.org/10.1007/s11771-016-3314-7
17. Zhu Z, Li X, Qu N, Zhu D (2015) A hybrid process for complex-shaped parts electroforming. Int J Adv Manuf Technol 81(8):779–784. https://doi.org/10.1007/s00170-015-7233-9
18. Xue Z, Lei W, Wang Y, Qian H, Li Q (2017) Effect of pulse duty cycle on mechanical properties and microstructure of nickel-graphene composite coating produced by pulse electrodeposition under supercritical carbon dioxide. Surf Coat Technol 325:417–428. https://doi.org/10.1016/j.surfcoat.2017.07.017
19. Feng Z, Shao L, Du L, Wang L (2015) Threefold diffusion layer model for one kind of pulse reverse nanoelectroforming. J Comput Theor Nanosci 12:2259–2263. https://doi.org/10.1166/jctn.2015.4016
20. Wang ZX, Wang S, Yang Z, Wang ZL (2010) Influence of additives and pulse parameters on uniformity of through-hole copper plating. Trans Inst Met Finish 88(5):272–276. https://doi.org/10.1179/002029610X12791981507884
21. Chen Y, He W, Chen X, Wang C, Tao Z, Wang S, Zhou G, Moshrefi-Torbati M (2014) Plating uniformity of bottom-up copper pillars and patterns for IC substrates with additive-assisted electrodeposition. Electrochim Acta 120:293–301. https://doi.org/10.1016/j.electacta.2013.12.112
22. Xiao H, He H, Ren X, Zeng P, Wang F (2017) Numerical modeling and experimental verification of copper electrodeposition for through silicon via (TSV) with additives. Microelectron Eng 170:54–58. https://doi.org/10.1016/j.mee.2016.12.030

Publisher's note Springer Nature remains neutral with regard to jurisdictional claims in published maps and institutional affiliations.